Organic Electronics 60 (2018) 64–70

Contents lists available at ScienceDirect

Organic Electronics

journal homepage: www.elsevier.com/locate/orgel

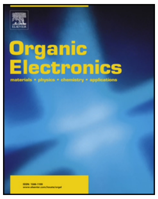

Efficient pure green light-emitting diodes based on formamidinium lead bromide perovskite nanocrystals

Lianwei Fan[a], Ke Ding[a], Hongting Chen[a], Songpo Xiang[a], Rui Zhang[a], Runda Guo[a], Zhitian Liu[b], Lei Wang[a,*]

[a] *Wuhan National Laboratory for Optoelectronics (WNLO), Huazhong University of Science and Technology, Wuhan 430074, People's Republic of China*
[b] *School of Materials Science of Technology, Wuhan, 430205, People's Republic of China*

ARTICLE INFO

Keywords:
Formamidinium lead bromide nanocrystals
Light-emitting diode
Concentration
Electroluminescence spectra
Recombination region

ABSTRACT

Formamidinium (FA) lead bromide (FAPbBr$_3$) perovskite nanocrystals (P-NCs) have ultrapure green emission and high stability, while FAPbBr$_3$ NCs based light-emitting diodes (FA-NLEDs) still have little report. Here, FAPbBr$_3$ NCs with a high photoluminescence quantum yield of 85.8% were synthesized. By controlling the concentration of FAPbBr$_3$ NCs in toluene solution, the exciton recombination region was precisely confined to the emitting layer and the parasitic emission coming from electron transport layer disappeared, resulting in the pure green emissions. The optimized FA-NLED presents a maximum external quantum efficiency (EQE), current efficiency (CE) of 3.84% and 16.08 cd/A respectively, with the EL emission peak of 528 nm, CIE of (0.183, 0.763) and a full width of half-maximum (FWHM) of 24 nm, which is among the best performance of FA-NLEDs.

1. Introduction

Recently, metal halide perovskite materials have attracted enormous attention, due to their excellent properties, such as low cost, high carrier mobility, high luminescent efficiency, adjustable wavelength, and narrow emission spectrum [1–3]. Metal halide perovskites light-emitting diodes (LEDs) based on solution-processed procedures was first reported in 2014 [4]. By interface engineering [5–7], optimizing the perovskite layer [8–11], controlling the crystallization process [12,13], and confining electrons and holes to two-dimensional perovskites [14–16], the external quantum efficiency (EQE) of perovskite polycrystalline films LEDs were promoted from 0.1% [4] to 14.36% [17]. However, the small exciton binding energy and defects induced low photoluminescence quantum yield (PLQY) of perovskite bulk materials which could limit their application in the LEDs [18–20]. Perovskite nanocrystals (P-NCs) are another form of potential peovskite luminescent material, whose grains size are smaller than 20 nm. They exhibit higher PLQY and larger exciton binding energy compared with perovskite bulk materials, which could realize high electroluminescence (EL) efficiency [21–23].

The most typical and outstanding representative P-NCs is metal lead bromide in luminescence field, and there are three major types in metal lead bromide P-NCs: methylamine lead bromide (MAPbBr$_3$) NCs, cesium lead bromide (CsPbBr$_3$) NCs and formamidinium (FA) lead bromide (FAPbBr$_3$) NCs. At present the PLQY of MAPbBr$_3$ NCs is as high as 90% [24], but methylamine ions are sensitive to heat, light, oxygen and humidity [25], leading to the instability of MAPbBr$_3$ NCs. CsPbBr$_3$ NCs is stable and can overcome the instability of MAPbBr$_3$ NCs, owing to the more stable inorganic cesium ions than organic ions [26,27]. Unfortunately, the emission wavelength of CsPbBr$_3$ NCs is always below 520 nm, caused by the small radius of cesium ion. Therefore, CsPbBr$_3$ NCs can't meet the requirements of the National Television System Committee (NTSC) and more recent Rec.2020 color standards for green emitter with the Commission International de l'Eclairage (CIE) color coordinates of (0.170, 0.797) [28]. Although the emission can be tuned to more than 520 nm by forming mixed halide perovskite (CsPbBr$_{3\text{-}x}$I$_x$) or adopting larger size of NCs, their PLQY and chemical stability are both sacrificed against fabricating highly efficient LEDs [22,29].

FAPbBr$_3$ NCs can easily achieve and maintain "525–535 nm" PL emission in comparison with CsPbBr$_3$ NCs, meeting the demands of standard green emitter without reducing PLQY [23,26]. Besides, compared with MAPbBr$_3$ NCs, FAPbBr$_3$ NCs are more stable. Especially the PLQY of FAPbBr$_3$ NCs reduced slightly from solution to film state [30]. However, rare endeavors have been made to develop the FAPbBr$_3$ NC-LEDs (FA-NLEDs) compared to LEDs of MAPbBr$_3$ NCs and CsPbBr$_3$ NCs. The first work about FA-NLED was reported in 2016 b y optimizing electron injection between different electron transport layers (ETLs), reaching a maximum CE of 6.4 cd/A [31]. And Young-Hoon Kim's group used surface ligand with a shorter carbon chain to enhance the charge injection, resulting in a maximum EQE of 2.05%, CE of 9.16 cd/

---

[*] Corresponding author.
E-mail address: wanglei@mail.hust.edu.cn (L. Wang).

https://doi.org/10.1016/j.orgel.2018.05.034
Received 20 April 2018; Received in revised form 23 May 2018; Accepted 24 May 2018

A [32]. The above researches illustrate that the charge transport is significant for improving the performance of FA-NLEDs, and the improved efficiency by optimizing the transport layer or the surface properties of NCs is limited and still need further improvement. Besides, there is no demonstration on charge injection management concerning the exciton recombination region in perovskite NCs emitting layer (EML), and the device performane can be further boosted with exciton recombination region controlling.

Here, we synthesized the bright $FAPbBr_3$ NCs and fabricated efficient perovskite light-emitting diodes (Pe-LEDs) by completely confining the exciton recombination region in EML. The recombination zone adjustment was managed through controlling the concentration of $FAPbBr_3$ NCs solution. With lower concentration of $FAPbBr_3$ NCs solution (thin $FAPbBr_3$ NC film, the recombination area in EML is narrow), hole transport is far more effective than electron and a parasitic emission at ETL side emerges. With increasing the NCs concentration (the recombination region in EML is expanding), the hole transport was reduced and excitons trend to recombine in NCs film. The excess emission in the EL spectrum gradually disappeared. Nevertheless, when the NC concentration further increases, though the exciton was completely limited to the EML, the transport of the carrier becomes very poor, resulting in the degradation of the device performance. The optimized efficient ultrapure green FA-NLED with the maximum CE of 16.08 cd/A, PE of 12.95 lm/W, EQE of 3.84%, CIE of (0.183, 0.763). To the best of our knowledge, it is among the highest efficiency of FA-NLEDs with three-dimensional (3D) $FAPbBr_3$ nanocrystals.

2. Experimental section

2.1. Materials

Oleylammonium bromide (OAmBr, ≥99.5% pure, from Xi'an Polymer Light Technology Corp.), Lead acetate trihydrate ($Pb(acetate)_2 \times 3H_2O$, 99.99%, from Aladdin-reagent), Formamidine acetate (FA-acetate, 99%, J&K Chemical Ltd), 1-octadecene (ODE, 90%, Sigma-Aldrich-reagent), oleic acid (OA, ≥99% pure Adamas-reagent), toluene and acetonitrile (from Sinopharm Chemical Reagent Co.,Ltd). Poly (3,4-ethylenedioxythiophene)/poly (styrenesulfonate) (PEDOT:PSS), Polyvinyl Carbazole (PVK) and 1,3,5-Tris (1-phenyl-1H-benzimidazol-2-yl)benzene (TPBi) (from Xi'an Polymer Light Technology Corp.), LiF (from Aladdin-reagent).

2.2. Synthesis and washing process of $FAPbBr_3$ nanocrystals

The $FAPbBr_3$ NCs were synthesized using hot-injection method [30]. FA-acetate (0.078 g, 0.75 mmol), $Pb(acetate)_2 \times 3H_2O$ (0.076 g, 0.2 mmol), dried OA (2 mL, vacuum-dried at 120 °C) and dried ODE (8 mL, vacuum-dried at 120 °C) were mixed in a 25 mL 3-neck flask and degassed under vacuum for 30 min at 50 °C. The mixture was heated to 130 °C under N_2, followed by the injection of OAmBr (0.21 g, 0.6 mmol) in toluene (2 mL). After 10 s, the reaction mixture was cooled to room temperature (below 20 °C) in an ice water bath. To the crude solution, 10 mL of toluene and 5 mL of acetonitrile were added and the mixture was centrifuged for 5 min at 12000 rpm. The supernatant was discarded and the precipitate was redispersed in 5 mL toluene. The toluene dispersion was centrifuged for 5 min at 11000 rpm, and the stably dispersed supernatant was collected. Acetonitrile was added into the toluene dispersion with a volume ration of 1:3. The acetonitrile and toluene mixture dispersion was centrifuged again at 11 krpm for 5 min, and the precipitate was collected and dispersed again in toluene. The process was repeated once more, the precipitate obtained after the last centrifugation was vacuum dried for 30 min to obtain the final product. The dried NCs powder dispersed in a certain amount of toluene to form a solution with different concentrations.

2.3. Device fabrication

Patterned indium tin oxide (ITO) coated glass with the sheet resistance less than 15 Ω/sq. was cleaned with alkaline leaner diluted with deionized water, deionized water, acetone, and isopropyl alcohol via ultrasonic cleaner for 60 min, 10 min, 30 min, 10 min, respectively, and then oven-dried for more than 2 h. The substrate was treated with oxygen plasma for 5 min before usage. PEDOT: PSS solution (Baytron P VPAl 4083, filtered through a 0.22 μm filter) was spin-coated onto the ITO-coated glass substrates at 2000 rpm for 60 s and baked at 120 °C for 30 min. The hole transporting layer (HTL) was prepared by spin-coating PVK chlorobenzene solution with the concentration of 8 mg/mL at 4000 rpm for 1 min and baked at 170 °C for 30 min $FAPbBr_3$ NCs were deposited by spin-coating at 1000 rpm for 50 s. Meanwhile, the NC layers annealed at 50 °C for 1 min, and then dried under vacuum for 30 min at room temperature. TPBi (40 nm) and LiF/Al electrodes (1 nm/100 nm) were deposited using a thermal evaporation system through a shadow mask under a high vacuum of $\approx 4 \times 10^{-4}$ Pa. The device active area was 9 mm^2 as defined by the overlapping area of the ITO and Al electrode.

2.4. Characterization techniques

The transmission electron microscope (TEM) image was measured using a Tecnai G2 20 U-Twin high-resolution scanning TEM operated at the accelerating voltage of 200 kV. The absorption spectra was obtained by a Shimadzu UV-3600 ultraviolet-visible-near-infrared (UV-vis-NIR) spectrophotometer. The PL spectra was measured through an Edinburgh FLS920 fluorescence spectrometer. The PLQYs of films were gained directly by a FLS920 steady state fluorescence spectrophotometer (Edinburgh Instruments C0., UK). The time-resolved PL decay was measured utilizing time-correlated single-photo counting by Edinburgh FLS920 with a 375 nm laser. X-ray diffraction (XRD) profile of as-prepared sample was measured using a PANalytical PW3040-60 materials research diffractometer, X-ray diffractometer. Atomic force microscopy (AFM) images were characterized using a Veeco Dimension 3100 NanoScope in a tapping mode measured by Bruker RTESPA-300 probes. The thicknesses of the films were measured by a Bruker DektakXT profilometer. The FA-NLEDs Performance data measurement were conducted using a Keithley 2400 source measurement unit and a Photo Research spectroradiometer (PR655). Ultraviolet photoelectron spectroscopy (UPS) spectra was collected on Kratos AXIS-ULTRA DLD-600 W using a helium discharge lamp ($h\nu = 21.2$ eV).

3. Results and discussion

$FAPbBr_3$ NCs were synthesized via a modified hot-injection synthetic method [30]. For simplicity, FA-Pb precursor solution was prepared by reacting FA and Pb acetates (0.75 and 0.2 mmol, respectively) with OA (2 mL) in ODE (8 mL). OAmBr (0.6 mmol, dissolved in 2 mL toluene) was injected into the mixture at 130 °C. The $FAPbBr_3$ NCs were cooled to room temperature after 10 s and purified twice that using toluene and acetonitrile as a solvent and nonsolvent, respectively.

The UV − vis absorption and (photoluminescence) PL spectrum of the $FAPbBr_3$ NCs in toluene solution are shown in Fig. 1a. The absorption edge is located at around 540 nm. The optical bandgap is determined as 2.3 eV. A strong PL peak at 525 nm was recorded excitated at 400 nm and the maximum half full width (FWHM) is narrow about 24 nm, satisfying the requirements of the NTSC more recent Rec.2020 color standards for green emitter [30]. The inset of Fig. 1a shows the typical transmission electron microscopy (TEM) image of $FAPbBr_3$ NCs, indicating the monodisperse cubic-shaped $FAPbBr_3$ NCs with the average edge length of 8–10 nm. Fig. 1b illustrates the X-ray diffraction (XRD) patterns of $FAPbBr_3$ NCs film. It shows that the diffraction peaks with the 2θ values on $FAPbBr_3$ NCs centered at around 14.6°, 20.9°, 29.6°,33.3°, 36.8°, 42.6°and 45.1°, and they correspond to the (100),